Compression After Impact Testing of Sandwich Structures Using a Four Point Bend Test

Alan T. Nettles, Justin R. Jackson
NASA Marshall Space Flight Center
Huntsville, AL 35812

Thomas S. Gates*
NASA Langley Research Center
Hampton, VA 23681

ABSTRACT

For many composite laminated face sheet sandwich structures, the design is driven by data obtained from compression after impact (CAI) testing. There currently is no universal standard for CAI testing of sandwich structures although there is one for solid laminates of a certain thickness and lay-up configuration. Most sandwich structure CAI testing has followed the basic technique of this standard where the loaded ends are precision machined and placed between two platens and compressed until failure. If little or no damage is present during the compression tests, the loaded ends may need to be potted to prevent end brooming. By putting a sandwich beam in a four point bend configuration, the region between the inner supports is under a compressive load and a sandwich laminate can be tested in this manner without the need for precision machining. Also, specimens with no damage can be taken to failure without specimen modification so direct comparisons between damaged and undamaged strength using the exact same test can be made. Data is presented for the four point bend CAI testing of various 8-ply quasi-isotropic face sheet sandwich panels and one type of these panels is compared with data from the more traditional end loaded CAI tests.

KEY WORDS: Damage Tolerance, Impact Damage, Testing

1. INTRODUCTION

Sandwich structures have been used in aircraft for many years and are currently being considered as primary load carrying components for manned spacecraft. With the use of sandwich structures as primary load bearing components comes a need to assess the compression-after-impact (CAI) strength of sandwich structures. With laminated composites it is well known that a low velocity impact may reduce the composite's compressive strength [1]. While other mechanical properties may also be reduced by an impact event, a composite's compression strength is the most susceptible due to the delaminations that can form causing local instability and premature failure.

* Deceased

CAI strength needs to be determined from testing which can be costly due to the high loads needed (large capacity test frame) and the specimen needing precision machining and strain gaging if the load is introduced into the sandwich specimen via end loading. One method of inducing a compressive load into a composite laminate is by utilizing a four-point-bend test on sandwich structure in which the "top" face sheet is in compression whilst the other face sheet is in tension. The bottom face sheet can be made such that it will not fail in tension before the top face sheet fails in compression. ASTM D 5467/D 5467M is a standardized method to test the compression strength of laminates by utilizing a sandwich structure.

Impacting sandwich panels and then subjecting them to four-point bending to put the damage zone in a "uniform" state of compression has been performed in the past [2-7]. In most of these tests, high density core had to be spliced into the sandwich panel outside of the upper span (gage length) so that the core did not fail in shear. The section under the upper span experiences no shear, so utilizing the actual density of core that will be used on the final structure is preferred to preserve the impact characteristics of the structure. In addition, these beams may need to be long to induce a large enough bending moment to cause the upper face sheet to fail in compression. By using a four point bend CAI test to eliminate the high loads and special specimen machining and strain gauging needed may get the cost of testing the CAI strength of composite sandwich structures down and more simple to perform, especially if one does not have access to a high capacity load frame. The relatively long specimen size that is needed for thicker or stronger face sheets is a drawback.

2. TESTING CONSIDERATIONS

2.1 Classical Assumptions For the following derivation, the discreet layers (laminae) of each face sheet are not considered, but rather the face sheet is treated as a "smeared" material with the laminate in plane modulus assumed to be the same through the thickness of each face sheet. This is valid for a face sheet that is "thin" compared of the core thickness; however, section 2.2 will introduce some unique concepts about this test geometry.

A schematic of a 4-point bend specimen is shown in Figure 1.

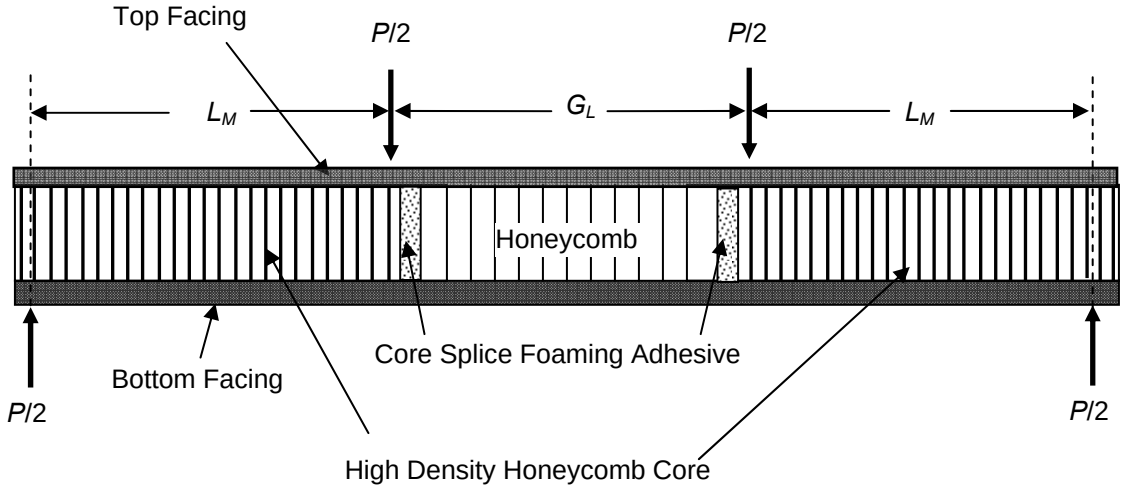

Figure 1. Schematic of four point bend test.

Where;
P = Total load applied to the specimen
L_M = Length of moment arm
G_L = Span length of upper supports (gage length)

A cross-sectional view through the center of the beam is shown in Figure 2.

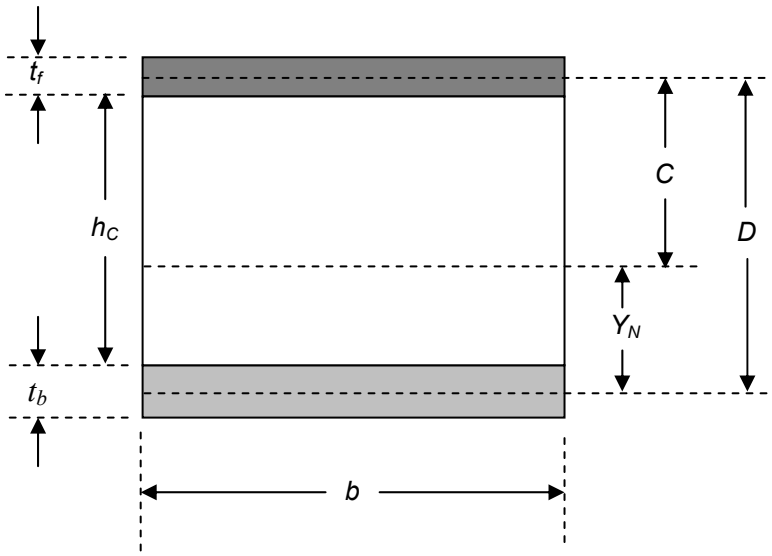

Figure 2. Cross Section of beam through its center.

Where;
t_f = thickness of the top face sheet
t_b = thickness of bottom face sheet
b = width of specimen
h_C = thickness of core
Y_N = distance from the center of the bottom face sheet to the neutral axis of the beam
$D = h_C + t_f/2 + t_b/2$

If the facings are of different modulii, then the bottom facing can have its width adjusted by the ratio of the bottom facing modulus to the top facing modulus and the facings can then be treated as the same material (the upper facing). Thus the "width" of the bottom face sheet is $(E_b/E_f)b$. Assuming the honeycomb core carries negligible tensile and compressive loads, the distance Y_N can be found from;

$$Y_N = \frac{y_f a_f + y_b a_b}{a_f + a_b} \tag{1}$$

Where the subscripts f and b represent the two face sheets and y is the distance from a horizontal reference line (typically the center of the bottom face sheet) and the center of a face sheet, and a is the cross-sectional area of a face sheet. Thus;

$$Y_N = \frac{Db\,t_f + 0(E_b/E_f)b\,t_b}{b\,t_f + b(E_b/E_f)t_b} = \frac{D\,t_f}{t_f + (E_b/E_f)t_b} \tag{2}$$

The stress in the middle of the top face sheet at a distance C from the neutral axis can be calculated from:

$$\sigma_f = \frac{MC}{I} \tag{3}$$

Where;
σ_f = Stress at the midplane of the upper face sheet.
M = Bending moment at the center of the beam.
C = Distance from neutral axis to center of top face sheet.
I = Moment of inertia of the beam about its neutral axis.

The bending moment is given by;

$$M = L_M(P/2) \tag{4}$$

The distance C is given by;

$$C = (D - Y_N) \tag{5}$$

The moment of inertia (assuming the core carries negligible tensile or compressive loads) is given by;

$$I = \frac{1}{12}b\,t_f^3 + (D - Y_N)^2\,b\,t_f + \frac{1}{12}b(E_b/E_f)t_b^3 + (Y_N)^2\,b(E_b/E_f)t_b \tag{6}$$

Assuming the face sheets are relatively thin, the t_f^3 and t_b^3 terms can be neglected and (6) becomes;

$$I = (D - Y_N)^2\,b\,t_f + (Y_N)^2\,b(E_b/E_f)t_b = b\left[(D - Y_N)^2\,t_f + (Y_N)^2(E_b/E_f)t_b\right] \tag{7}$$

Thus the stress at the midplane of the top face sheet is given by putting (4), (5) and (7) into (3);

$$\sigma_f = \frac{L_M(P/2)(D - Y_N)}{b\left[(D - Y_N)^2\,t_f + (E_b/E_f)(Y_N)^2\,t_b\right]} \tag{8}$$

2.2 Strain Variation Within the Face Sheet It should be noted that there will be a variation in compressive strain within the plane of the upper face sheet from its lower surface to its top surface. Figure 3 shows the compressive strain variation through the thickness of the top face sheet of a sandwich panel. At the top of the upper face sheet, the distance to the neutral axis of the beam is C+t_f/2 and at the bottom of the upper face sheet the distance is C+t_f/2. Thus if the

compressive strain at the outer fibers (top) of the upper face sheet is denoted by ε_{max} and the stress at the lower fibers (next to the core) denoted by ε_{min}, then;

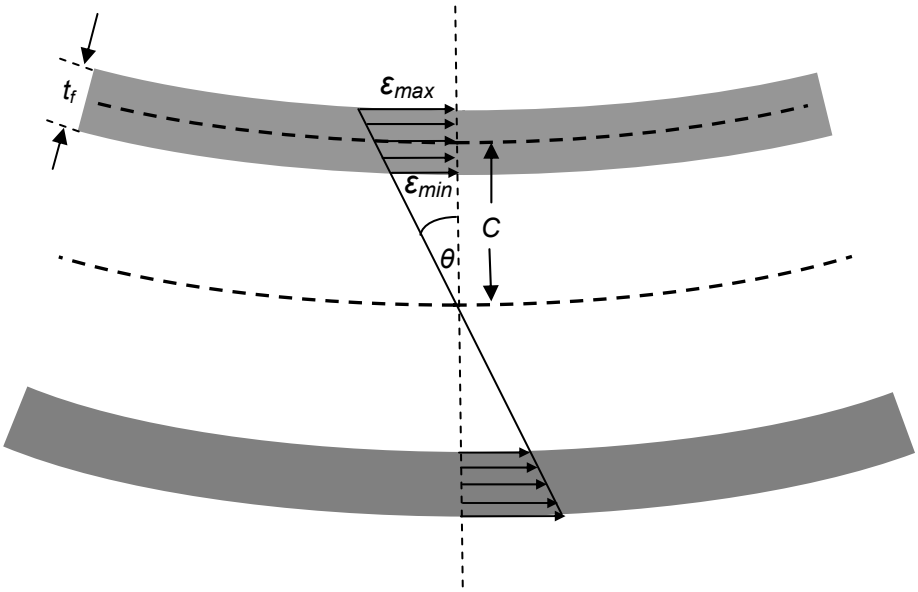

Figure 3. Strain gradient through face sheet due to bending.

From the geometry;

$$\varepsilon_{\min} = \left(C - \frac{t_f}{2} \right) \tan\theta \qquad \text{and} \qquad \varepsilon_{\max} = \left(C + \frac{t_f}{2} \right) \tan\theta \tag{9}$$

The percent increase from ε_{min} to ε_{max} is given by;

$$\%\Delta = (100)\frac{\varepsilon_{\max} - \varepsilon_{\min}}{\varepsilon_{\min}} \tag{10}$$

Putting (9) into (10) gives;

$$\%\Delta\varepsilon = (100)\%\frac{\left(C + \frac{t_f}{2} \right)\tan\theta - \left(C - \frac{t_f}{2} \right)\tan\theta}{\left(C - \frac{t_f}{2} \right)\tan\theta} = (100)\%\frac{t_f}{C - t_f/2} \tag{11}$$

For the difference through the thickness of the upper face sheet Figure 4 plots $\%\Delta\varepsilon$ as a function of h_C assuming an upper face sheet thickness of 2.03 mm (a typical 16-ply laminate) and t_f/t_b face sheet ratios of 1.0, 0.5 and 0.33 using equation (11).

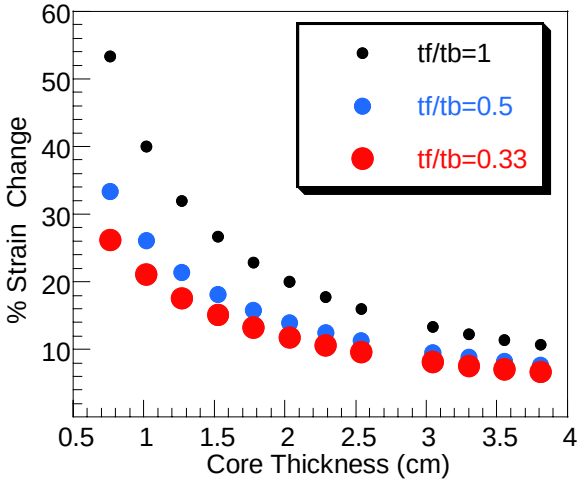

Figure 4. Plot of % difference of strain through top face sheet versus core thickness for various t_f/t_b ratios.

Figure 4 indicates that even with thick core, the percent difference in strain through the laminate may be significant. It is also seen that the thicker the bottom face sheet, the less severe the stress gradient through the thickness of the top face sheet (for a given core thickness). Thus for obtaining a more uniform stress through the thickness of the top face sheet, a thick bottom face sheet is desired and/or a thicker core is also desired. To observe the effects increasing these thicknesses cause to the developed stress in the upper face sheet, the maximum stress in the upper face sheet is plotted versus core thickness in Figure 5 for a given load of P=44.5kN (the upper limit of many common "bench top" load frames). Other variables were held constant at b=7.6 mm (the minimum width needed so the damage does not interfere with edge effects), L_M=10.2 mm (so as to not use more material than the end-loaded type specimens) and t_f=2.03 mm (the typical thickness of a 16-ply laminate). However, as the bottom face sheet becomes thicker, the stress developed in the upper face sheet become less as shown in Figure 5. Also, as the core gets thicker, the less stress is developed in the upper face sheet.

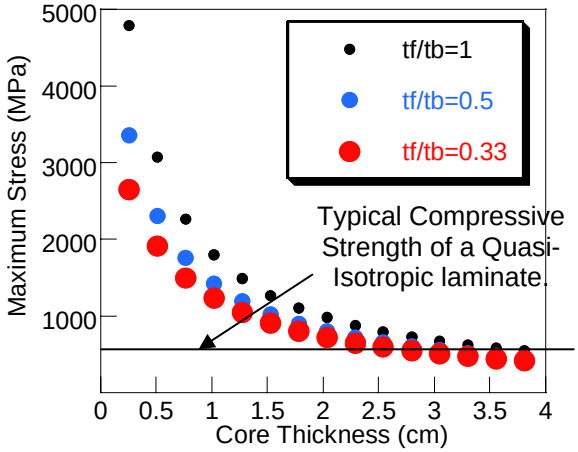

Figure 5. Maximum stress in the upper face sheet versus core thickness for various t_f/t_b ratios.

To examine the effects of using different materials (rather than changing thicknesses) for the top and bottom face sheet a plot of σ_{max} versus various E_b/E_f ratios is shown in Figure 6 for core thicknesses of h_C = 1.27,2.54 and 3.81 cm. Other variables are held constant at; t_f = 2.03 mm,

load P=44.5 kN, L_M=10.2 mm and b=7.6 mm for reasons mentioned earlier. The bottom face sheet is assumed to have the same thickness as the top face sheet.

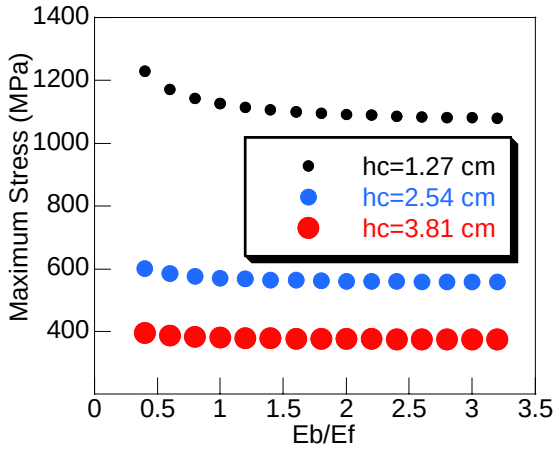

Figure 6. Maximum upper face sheet stress as a function of E_b/E_f ratios.

The Figure shows that if the bottom face sheet modulus is similar, or stiffer, than the top face sheet modulus, then the difference in stiffness of the face sheets does not significantly affect the stress in the upper face sheet, especially as the core gets thicker. Typically if an aluminum face sheet is used as the bottom face sheet (E = 69 GPa) and a quasi-isotropic laminate with high strength fibers is used as the top face sheet (E = 57 to 65 Gpa), then the differences in materials has very little influence on the calculated stress.

A satisfactory balance for core thickness needs to be decided upon since as the core gets thicker, the percent difference in stress through the thickness of the face sheet decreases, but the load needed to break the face sheet (for a given moment arm length, L_M) increases. An example of the increasing load to break the upper face sheet with increasing core thickness is shown in Figure 7 for an upper face sheet that breaks at σ_{max} = 517 Mpa (the typical compression strength of a quasi-isotropic laminate with intermediate modulus fibers).

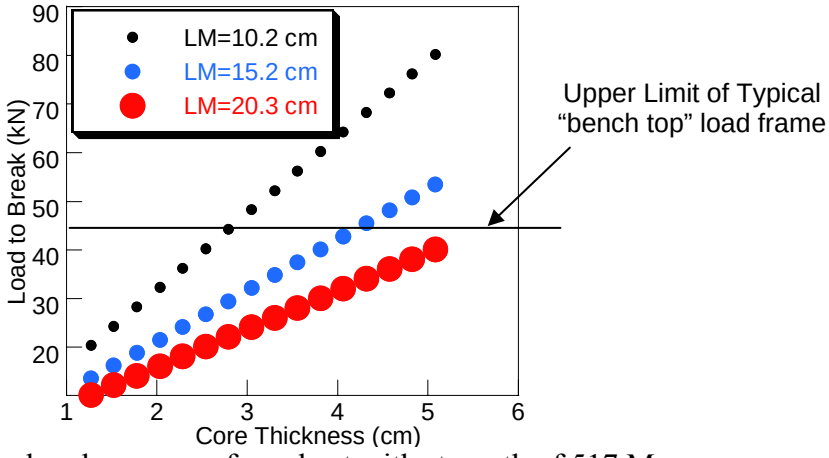

Figure 7. Load needed to break an upper face sheet with strength of 517 Mpa versus core thickness.

The face sheets are 2.03 mm thick (typical of a 16-ply quasi-isotropic laminate) and 3 different moment arm lengths are shown. Longer moment arms will allow a smaller capacity load frame to

be utilized, but will use more material. Thus a satisfactory balance between amount of material used and the maximum capacity of the load frame needs to be determined.

3. EXPERIMENTAL

3.1 Materials and Specimens The sandwich specimens used in this study were all composed of an aluminum honeycomb core one-half inch in thickness bonded to face sheets 7.6 cm wide and 35.6 inches in length. The top face sheets were 8 plies consisting of IM7/8552 0.127 mm thick prepreg laid up in a quasi-isotropic configuration. The nominal thickness of the 8-ply face sheet laminates was 1.02 mm. For the IM7/8552 specimens, the core had a density of 72 kg/m^3 in the center (to preserve the impact characteristics of the core intended for a specific project) and 193 kg/m^3 on the outside (to carry the high shear loads developed in this area) The bottom face sheet had a thickness of 1.05 mm and consisted of 5 plies of woven T300/934. Some of the IM7/8552 face sheets were co-cured with a lay-up configuration of $[0,+45,90,-45]_S$. Face sheets with a lay-up configuration of $[+45,90,-45,0]_S$ were both co-cured and procured. For the specimen geometry used in this study, a 32% change in strain from the inner fibers of the upper face sheet to the outer fibers of the upper face sheet can be expected.

For a comparison, some impacted panels of pre-cured IM7/8552 were cut into 13.3 X 26.0 cm specimens and end-loaded in compression to failure to compare to the 4 point bend results. These panels were tested at NASA's Langley Research Center (LaRC). A photograph of an end-loaded specimen loaded in the compression fixture is shown in Figure 8.

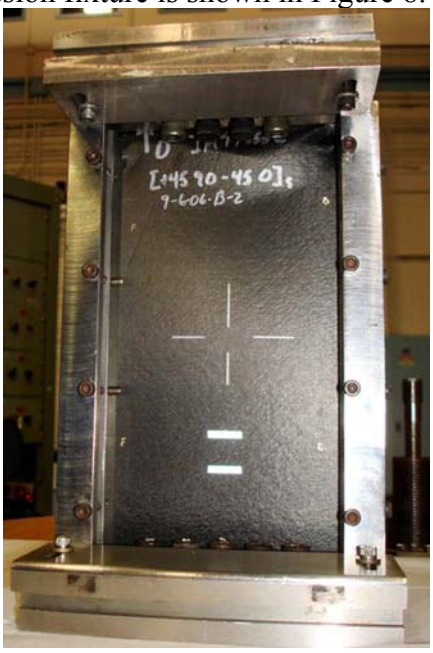

Figure 8. Picture of End-Loaded Compression Fixture and Test Panel

A summary of the core, face sheet, and cure type are given in Table 1 for the specimens used in this study.

Test Series	Face Sheet Material	Face Sheet Lay-Up	Cure Condition	Core Density in Gage Length (kg/m^3)	CAI Test Type	Number Tested
1	IM7/8552	$[0,+45,90,-45]_S$	Co-cure	72	4-pt. bend	46
2	IM7/8552	$[45,90,-45,0]_S$	Co-cure	72	4-pt. bend	16
3	IM7/8552	$[45,90,-45,0]_S$	Pre-cure	72	4-pt. bend	40
4	IM7/8552	$[45,90,-45,0]_S$	Pre-cure	72	End-compression	12

Table 1. Compression after impact test parameters

3.2 Impact Testing A drop weight tower was used to impact the sandwich specimens with a range of impact energies. The impact energy was varied by adjusting the height of the dropped weight. The impactor (tup) used in this study had a diameter of, 1.27 inches. The amount of weight used was 1.23 kg. The specimens were placed flat on a metal plate during impact since this was simple to perform and gave the most damage in the upper face sheet for a given impact energy as opposed to other boundary conditions. The specimens were non-destructively evaluated using flash thermography to determine the planar extent of damage.

3.3 Flash Thermography Testing The non-destructive evaluation (NDE) data was obtained via flash thermography, a technique which uses an ultra sensitive infared (IR) camera to detect the dissipation of heat from the specimen after it has been "flashed" with a bright light and thus given a burst of heat. An example of a flash thermography image is shown in Figure 9. The "damage size" used in the data reduction is shown. The "damage size" was the width of the circular shaped damage pattern detected.

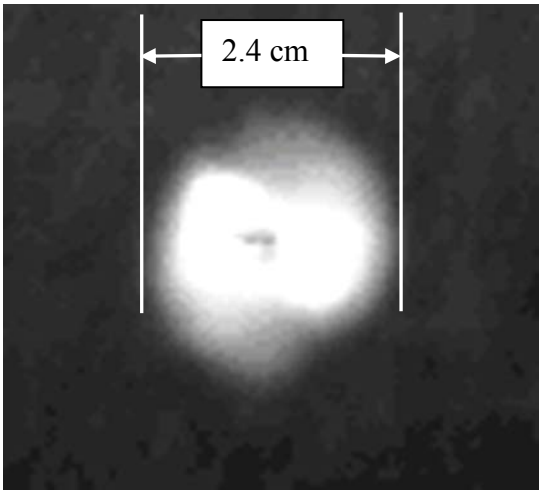

Figure 9. Example of a flash thermography image and its "damage size".

3.4 Four Point Bend Testing The four point bend tests were conducted per ASTM D 5467. In order not to crush the specimen under the four loading points, 2.54 cm long rubber pads (shown in red) with aluminum shims covering them were placed across the width of the specimen as shown in Figure 10. The horizontal loading rods were 2.54 cm in diameter.

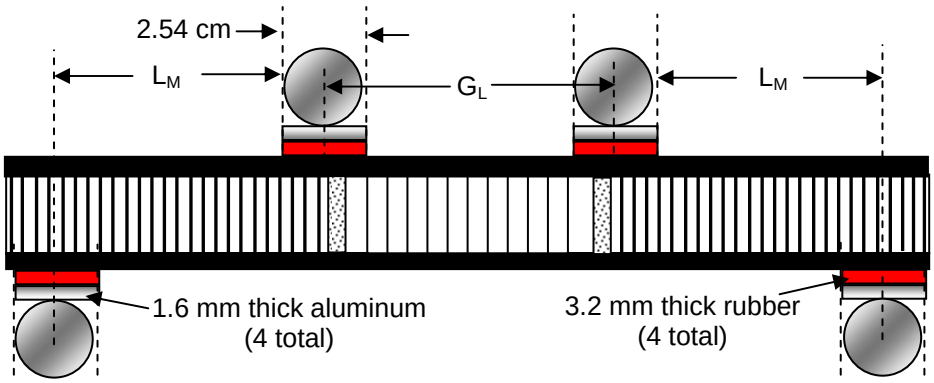

Figure 10. Loading pad placement on bending specimens to prevent localized crushing.

The load was assumed to act at the midline of each of the rubber pads. The specimens were loaded in 4 point bending with various lower spans ranging from 33.7 to 30.5 cm and an upper span of between 8.9 and 11.4 cm. Tests were performed on a 50 kN capacity electromechanical test frame. A photograph of a typical failed specimen is shown in Figure 11.

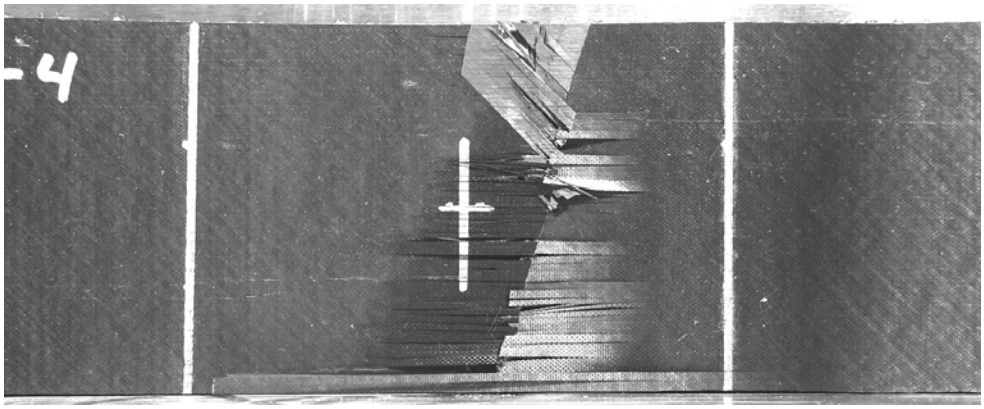

Figure 11. Photograph of typical failed four point bend specimen.

3.5 End-Compression Testing An end-compression test fixture was used at LaRC to evaluate CAI residual strength. The specimens for this fixture were nominally 26.0 X 13.3 inches (length X width). For these series of tests, the fixture was designed to provide a uniform end compressive load while providing simple support boundary conditions along the length. The test specimen and fixture used in these tests is shown in the photograph in Figure 8. Tests were performed in a 250 kN servo-hydraulic test machine with compression platens placed in the upper and lower grips. Longitudinal front and back strain was measured away from the impact site using non-contacting laser extensometers in order to determine panel bending due to misalignment or impending failure. In order to avoid end crushing, specimens were stiffened in the first 3.8 cm of each end using a fast-cure epoxy poured into a gap milled between face sheets. Specimen ends were then milled flat and parallel after the epoxy cured and set. A photograph of a typical failed specimen is shown in Figure 12.

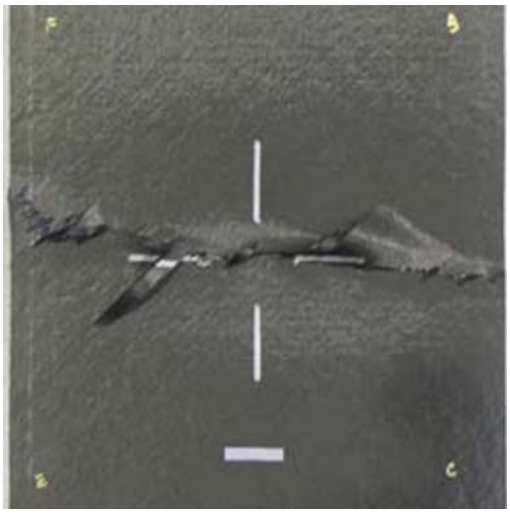

Figure 12. Photograph of a typical end-loaded compression after impact specimen.

4. Results

The results will be separated out into each type face sheet tested and test method. Comparisons will be made after showing all of the data separately. The compression strength data represents the maximum (outer fiber) stress in the face sheet.

4.1 IM7/8552 Co-Cured $[0,+45,90,-45]_S$ Face Sheets; (Test Series 1) These specimens had an upper face sheet lay-up of $[0, +45, 90, -45]_S$ and were co-cured to 72 kg/m^3 aluminum honeycomb core with FM-1000 film adhesive. The bottom face sheet consisted of 5 plies of woven T300/934 with a bi-directional lay-up. The panels were cured at 275 kPa and 176ºC. All of these specimens were impacted with a 1.27 cm diameter tup. These specimens were non-destructively evaluated with flash thermography and the results are given as the diameter of the circular planar area of damage as detected from the images. The CAI results are plotted versus NDE size in Figure 13.

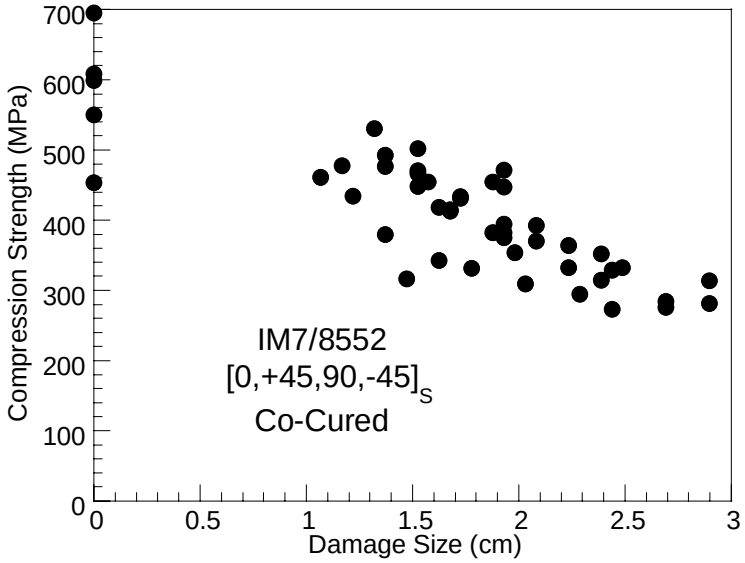

Figure 13. Compression after impact versus damage size for IM7/8552 $[0, +45, 90, -45]_S$ co-cured specimens tested utilizing the 4-pt. bend test.

4.2 IM7/8552 [+45, 90, -45, 0]$_S$ Face Sheets; (Test Series 2 and 3) These specimens had an upper face sheet lay-up of [45, 90, -45, 0]$_S$ A total of 16 were co-cured to 72 kg/m^3 aluminum honeycomb core with FM-1000 film adhesive and 74 were pre-cured and then secondarily bonded to 72 kg/m^3 core with 777-1. The bottom face sheet consisted of 5 plies of woven T300/934 with a bi-directional lay-up. The panels were cured at 275 kPa and 176ºC. These specimens were impacted with a 1.27 cm diameter tup. These specimens were non-destructively evaluated with flash thermography and the results are given as the diameter of the circular planar area of damage as detected from the images. The CAI results are plotted versus NDE size in Figure 14.

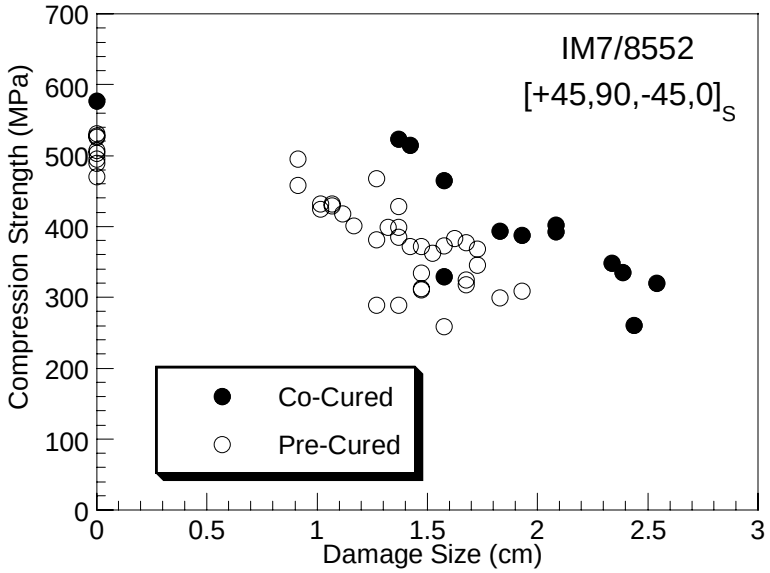

Figure 14. Compression after impact versus damage size for IM7/8552 [+45,90,-45,0]$_S$ specimens tested utilizing the 4-pt. bend test.

4.3 End-Compression IM7/8552 [+45, 90, -45, 0]$_S$ Face Sheets (Test Series 4)

These specimens were end loaded and had identical facings with a lay-up of [+45, 90, -45, 0]$_S$. A total of 12 were precured and then secondarily bonded to 4.5 lb/ft^3 core with 777-1. The panels were cured at 275 ksi and 176ºC. These specimens were impacted with a 1.27 cm diameter tup. These specimens were non-destructively evaluated with flash thermography and the results are given as the diameter of the circular planar area of damage as detected from the images. The CAI results are plotted versus NDE size in Figure 15.

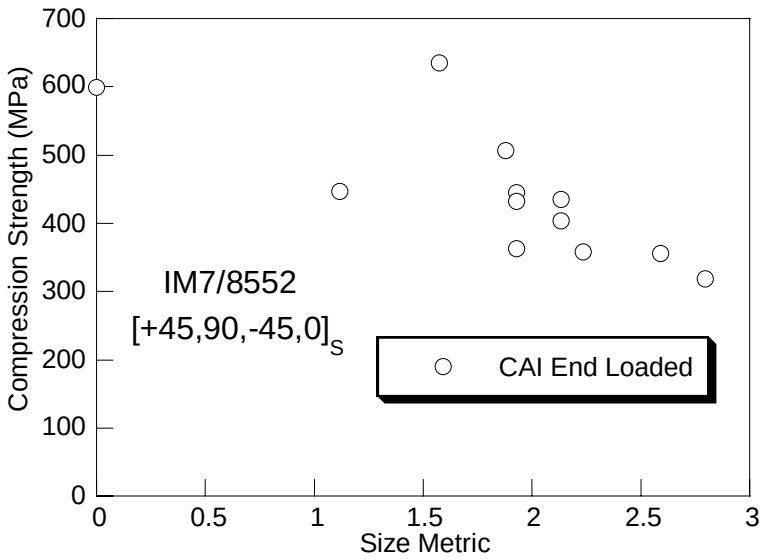

Figure 15. Compression after impact versus damage size for end-loaded specimens.

5. Comparisons

Some comparisons of the test type, lay-up and pre versus co-cure will be examined in this section.

5.1 Test Type A comparison of the pre-cured IM7/8552 $[+45,90,-45,0]_S$ specimens tested using the 4-point bend and the end loaded method are shown in Figure 16.

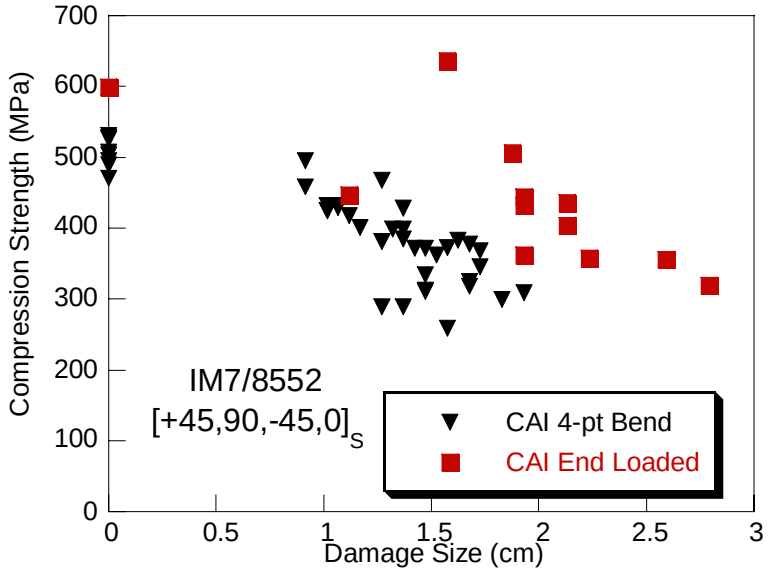

Figure 16. Comparison of CAI vs. Damage Size Data for End Loaded and 4-pt. bend specimens.

The end-loaded test specimens generally gave a higher compression strength for a given damage size. Although only one undamaged specimen was taken to failure via the end-loading method, this value was higher than any of the four point bend specimens. Reasons for the difference are mainly found in the four point bend tests. Assumptions are made in developing equation (8) which may not be valid for the relatively thin (1.27 cm) honeycomb used in this study, the assumption that all of the applied load acts in a line at the center of each of the 4 rubber "load spreader" pads may not be valid and the 32% strain gradient through the face sheet thickness may be part of the reason.

5.2 $[0,+45,-45,90]_S$ versus $[+45,90,0,-45]_S$ Lay-up Figure 17 shows the CAI data plotted as a function of NDE size and Impact energy. When compared on the basis of NDE size, there appears to be little to no difference.

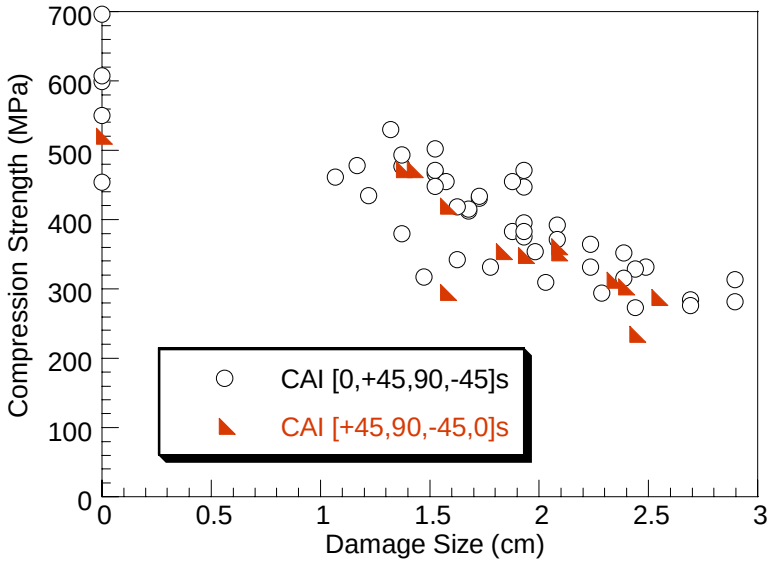

Figure 17. CAI strength versus damage size for two co-cured lay-up configurations tested in 4-pt. bend.

Thus the CAI data are comparable if based on damage size as the dependent variable and the lay-up cannot account for the differences between test methods seen in the previous section.

5.3 Co-Cured Versus Pre-Cured An examination of Figure 14 shows that the co-cured specimens generally have higher compression strengths when plotted against the damage size as measured by NDE. The co-cured data from the $[0,+45,90,-45]_S$ specimens can be included since the previous section showed that lay-up was irrelevant when using damage size. The co-cured versus pre-cured data with all lay-ups is shown in Figure 18.

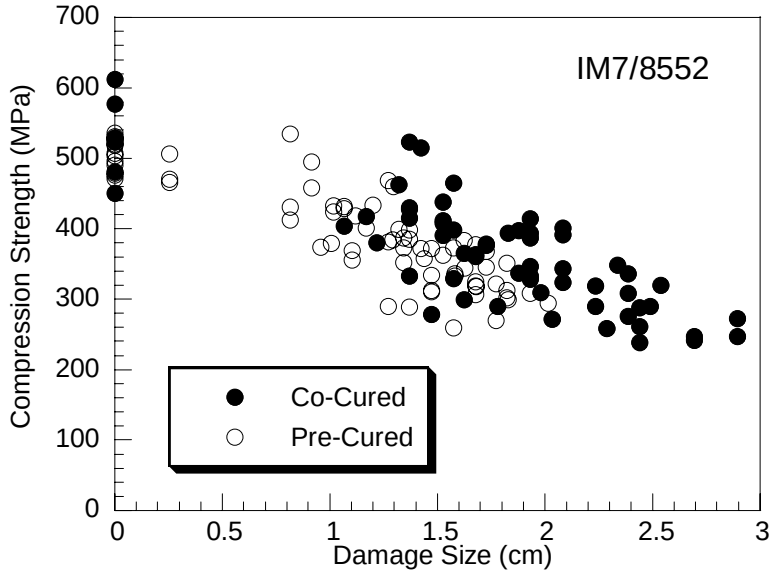

Figure 18. CAI data for co-cured and pre-cured IM7/8552 tested utilizing the 4-pt. bend test.

The undamaged strengths are about the same which is unexpected since the "waviness" of the plies closest to the honeycomb should reduce the compression strength of the laminate. When damage is present, the co-cured specimens trend towards the higher end of strength.

6. Conclusions

Utilizing a four point bend test to generate compression-after-impact (CAI) data is a viable alternative to end loading type testing. The advantages of the four point bend test are that smaller loads can be used to generate the breaking stress and the specimen need not be precision machined and strain gaged. The disadvantages, as shown in this study, are that there is a non-uniform stress state through the thickness of the face sheet and long specimens will probably be needed. Also, the CAI results show that the end-loaded specimens gave slightly higher failure stresses. This could be from the assumptions used for the stress equation for the 4-point bend specimens. Strain gages could be placed on the four point bend specimens to get a direct reading, but this defeats one of the advantages of using the four point bend tests. Thus unless material is plentiful and there is no access to a large capacity load frame, the end loading method is preferable.

7. References

1. S. Abrate., "Impact on Laminated Composites: recent Advances," Applied Mechanics Review, 47, pp. 517-544 (1994).
2. M.D. Rhodes, "Impact Fracture of Composite Sandwich Structures", AIAA Paper No. 75-748, (1975).

3. T. Gottesman, M. Bass, and A. Samuel in F.L. Matthews, ed., Proceedings of the 6th International Conference on Composite Materials, Elsevier Applied Science, London and New York, 1987, pp. 3.27-3.35.
4. O. Ishai and C. Hiel, "Damage Tolerance of a Composite Sandwich with Interleaved Foam Core," Journal of Composites Technology and Research, 14, pp. 155-168, (1992).
5. A. Nettles, D. Lance and A. Hodge, "A Damage Tolerance Comparison of 7075-T6 Aluminum Alloy and IM7/977-2 Carbon/Epoxy," SAMPE International Sympossium, 36, pp. 924-931, (1991).
6. A. Nettles and D. Lance, "A Study of the Damage Tolerance Enhancement of Carbon/Epoxy Laminates By Utilizing an Outer Lamina of Ultra High Molecular Weight Polyethylene," SAMPE International Technical Conference, 23, pp. 62-71, (1991).
7. M. Raju et. al., "Repair Effectiveness Studies on Impact Damaged Sandwich Composite Constructions," Journal of Reinforced Plastics and Composites, 25, pp. 5-16, (2006).